Dynamic Reconfiguration of Photovoltaic Energy Harvesting System in Hybrid Electric Vehicles

Yanzhi Wang[1], Xue Lin[1], Naehyuck Chang[2], and Massoud Pedram[1]
[1]Department of Electrical Engineering, University of Southern California, Los Angeles, CA, USA
[2]Seoul National University, Seoul, Korea
[1]{yanzhiwa, xuelin, pedram}@usc.edu, [2]{naehyuck}@elpl.snu.ac.kr

ABSTRACT
Photovoltaic (PV) energy harvesting system is a promising energy source for battery replenishment in hybrid electric vehicles (HEVs.) The PV cell array is installed on different parts of a vehicle body such as the engine hood, door panels, and the roof panel. Non-uniformity of the solar irradiance and temperature on the PV cell array is, however, a serious obstacle to efficient utilization of the PV system in HEVs because such variation, if not managed properly, can result in a significant degradation in the overall output power level of the PV system. This paper presents a dynamic PV array reconfiguration technique with structural support and a dynamic programming-based algorithm with polynomial time complexity to produce the near-optimal reconfiguration of the PV array on the HEV. The goal of this technique is to maximize the PV system output power under any solar irradiance and temperature distribution on the PV array. We demonstrate up to 6X improvement in the output power of a PV system against a conventional fixed configuration PV system.

Categories and Subject Descriptors
B.8.2 [**Performance and Reliability**]: Performance Analysis and Design Aids.

General Terms
Algorithms, Design, Management, Performance.

Keywords
Photovoltaic System, Hybrid Electric Vehicle, Photovoltaic Array Reconfiguration, Dynamic Programming.

1. INTRODUCTION
With growing public consciousness about the greenhouse gas emissions and increase in the price of petroleum, hybrid electric vehicles (HEVs) are perceived as a core segment of future automotive market. HEVs employ both electric motors and internal combustion engines to improve the fuel economy. Batteries powering the electric motor in a HEV must be recharged by a generator in the HEV. On top of a regenerative braking-based battery charging scheme, a photovoltaic (PV) system mounted on the HEV can enable battery charging whenever there is solar irradiance. PV cells can be mounted on the roof panel, engine hood, trunk, and door panels of a HEV.

PV systems have been widely deployed for many applications since solar energy is abundant, renewable, and clean. A PV system consists of a PV array and peripheral charging regulation circuitry (e.g., the charger). A PV array itself comprises multiple PV cells connected in a series-parallel configuration. Ideally, all PV cells in the array experience identical operational conditions and exhibit the same voltage-current (V-I) and voltage-power (V-P) output characteristics. Thus, they can simultaneously operate at their *maximum power points* (MPPs.) We can achieve the maximum output power of the PV array with a *MPP tracking* (MPPT) method [1][2]. Furthermore, the recently proposed *maximum power transfer tracking* (MPTT) technique can guarantee the maximum output power of the PV system under non-ideal behaviors of the charger [3]. In reality, PV cells may receive different solar irradiances due to *partial shading* and variations in the *solar irradiance incidence angle*. In addition, PV cells may experience different temperatures. For instance, PV cells on the door panel have a different solar irradiance incidence angle from those on the roof. PV cells on top of the hood have a higher temperature than PV cells on the roof.

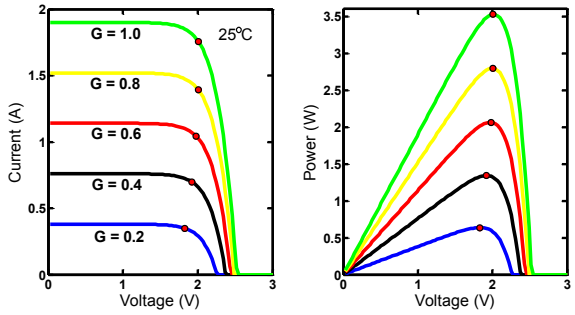

Figure 1. V-I and V-P characteristics of a PV cell under different solar irradiances.

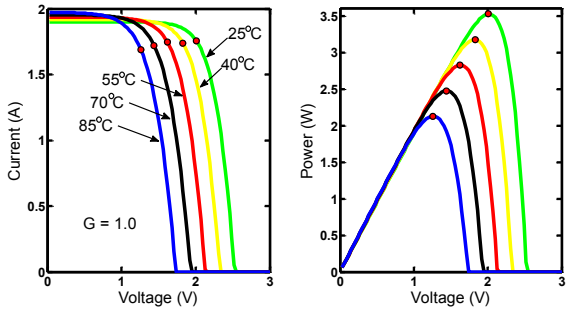

Figure 2. V-I and V-P characteristics of a PV cell under different temperatures.

Figures 1 and 2, where MPPs of a PV cell are marked by red dots, illustrate that a higher solar irradiance or a lower temperature lead to a higher output power at the MPP of the cell. Partial shading not only reduces the maximum output power of the shaded PV cell, but also makes non-shaded PV cells that are connected in series with the shaded one deviate from their MPPs.

ISLPED'12, July 30– August 1, 2012, Redondo Beach, California, USA.

Similarly, a hotter PV cell makes PV cells that are connected in parallel with it deviate from their MPPs. Thus PV cells in a PV array with solar irradiance and/or temperature non-uniformity cannot operate at their MPPs simultaneously, and thus, the PV array suffers from significant power inefficiency. In addition, the V-P characteristic curve of such a PV array shows multiple peaks. Therefore, the existing MPPT or MPTT techniques, which are based on the unimodality assumption of V-P characteristics, have to be modified to find the global optimal operating point of the PV array [4][5]. This fact increases the complexity of the PV system controller. Some PV array reconfiguration techniques have been proposed [6][7][8] to solve the PV system power loss problem due to solar irradiance and temperature non-uniformity phenomenon. These techniques suffer from the following shortcomings: i) they require extra PV cells to perform reconfiguration; ii) a systematic and scalable reconfiguration control mechanism is lacking; and iii) they do not consider charger efficiency variation in the PV system.

In this paper, we present a dynamic PV array reconfiguration technique, which updates the PV array configuration according to the change of irradiance and temperature distribution on the PV array during system operation in order to enhance the output power of PV systems. Our reconfiguration technique has the ability to simultaneously meet (to the extent that is possible) the MPPs for all PV cells even under non-uniform solar irradiance and temperature distributions. We provide both a scalable structural support and an effective control algorithm. The control algorithm realizes near-optimal PV array reconfiguration accounting for solar irradiance and temperature distributions and charger efficiency variation. The algorithm is based on dynamic programming with polynomial time complexity so that it can be integrated into PV systems with insignificant computational overhead. Experimental results demonstrate that our proposed dynamic reconfiguration technique results in up to 6X improvement in PV system output power compared with a conventional fixed array structure PV system.

2. PV SYSTEM MODEL AND RECONFIGURATION

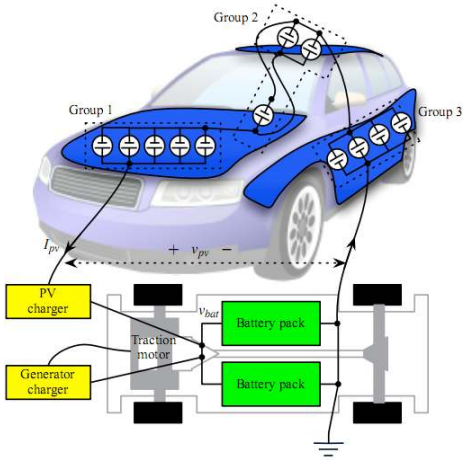

Figure 3. System diagram of a PV-powered HEV.

Figure 3 shows the system diagram of a PV-powered HEV. The PV array consists of a number of PV cells, mounted on the roof panel, engine hood, trunk, and door panels of the HEV. Conventional HEVs are equipped with battery packs as the energy storage system, connected to the traction motor via the generator charger. The PV-powered HEV also has an add-on PV system that consists of a PV array and a PV charger connecting the PV array to battery packs. The generator charger and PV charger can simultaneously charge battery packs. MPPT or MPTT techniques are integrated with the PV charger, and therefore, the PV charger can set the optimal operating point for the PV array. The PV array consists of a number of series-connected PV cell groups where each PV group consists of (potentially a different number of) PV cells connected in parallel. Although mounting positions of PV cells are fixed on the HEV, PV array reconfiguration technique adaptively changes the electric connection of PV cells in response to changes in the environmental condition. Figure 4 provides the equivalent circuit of the PV system shown in Figure 3, where the battery bank in Figure 4 represents the battery packs on HEV.

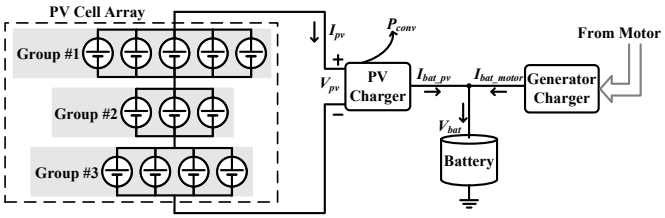

Figure 4. Equivalent circuit of a PV system on a HEV.

2.1 Component Models

It is necessary to have accurate component models, including models for the PV cell, battery and charger, in order to develop an effective PV array reconfiguration algorithm. Given the solar irradiance G and temperature T of a PV cell, the PV cell voltage V_{pv}^c and current I_{pv}^c satisfy certain V-I characteristics as shown in Figures 1 and 2. The MPP (maximum power point) that maximizes the PV cell output power $V_{pv}^c \cdot I_{pv}^c$ lies on the V-I curve. In terms of the notation, we have: $V_{pv}^c = V_{pv}^{c,MPP}$ and $I_{pv}^c = I_{pv}^{c,MPP}$ at the MPP. We obtain the V-I characteristics and MPP of a PV cell under any (G, T) using the PV cell model of reference [10]. We adopt the battery and charger models from [11]. Generally speaking, the power conversion efficiency of a charger is a function of its input and output voltages and currents. The conversion efficiency is maximized when the charger output current is within a small operation range, and its input and output voltages are close to each other.

2.2 Reconfiguration Structure for PV Array

A conventional PV array consists of n series-connected PV groups, whereby each PV group has exactly m parallel-connected PV cells, (all PV groups have the same number of PV cells.) In contrast, the PV array in Figure 4 has three series-connected PV cell groups, and there are different numbers of parallel-connected PV cells within the groups, which is an imbalanced configuration. Reference [9] presented a structural support mechanism for balanced reconfiguration of supercapacitor banks. In this paper, we exploit the structural support in [9] for the PV array. However, we allow more flexible configurations (both balanced and imbalanced) of PV cells in the PV array.

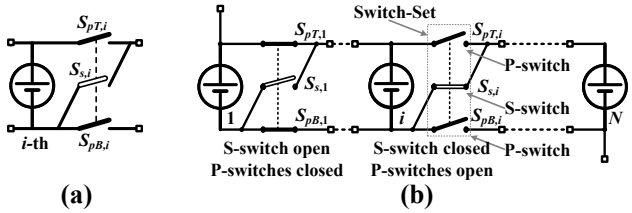

Figure 5. Reconfiguration structure.

We demonstrate the possibility of creating an imbalanced reconfiguration using the reconfiguration structure of [9]. The PV cells are integrated with a series switch S_s and a pair of parallel switches S_{pT} and S_{pB}, as shown in Figure 5 (a). The PV array has a reconfiguration structure as shown in Figure 5 (b), where the PV array consists of N PV cells and all the PV cells except for the last one are integrated with switches. We can realize PV array

reconfiguration by controlling the states of switches. For any PV cell, its two parallel switches are always in the same state, so we use $S_{p,i}$ to denote the pair of parallel switches in *i*-th PV cell of the array. $S_{p,i}$ is used for connecting the PV cells in parallel, and $S_{s,i}$ is used for connecting the PV cell groups in series. If $S_{p,i}$ is on, $S_{s,i}$ must be off; if $S_{s,i}$ is on then $S_{p,i}$ must be off. Figure 6 shows the states of switches to realize the imbalanced configuration shown in Figure 4, where group #1 is formed by turning on $S_{p,1}$ through $S_{p,4}$ to form a group of five parallel connected PV cells whereas groups #1 through #3 are series-connected by turning on $S_{s,5}$ and $S_{s,8}$.

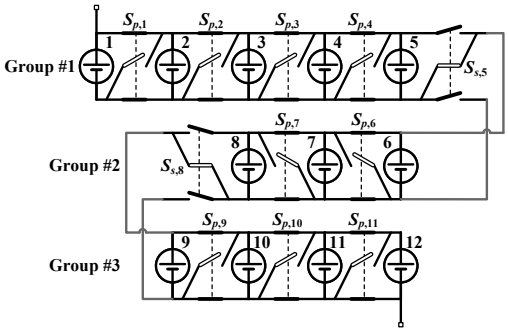

Figure 6. Example of imbalanced configuration.

In the PV array configurations achieved by the reconfiguration structure, the number of groups *n* in the PV array can be any positive integer less than or equal to *N*. The number of parallel-connected PV cells $m_j (> 0)$ in each group should satisfy

$$\sum_{j=1}^{n} m_j = N. \tag{1}$$

We denote such a configuration as $\mathcal{C}(n;\ m_1, m_2, \cdots, m_n)$, which could be viewed as a partition of the PV cell index set $\boldsymbol{A} = \{1, 2, \cdots, N\}$, where integers in $\boldsymbol{A}$ denote the indices of the PV cells in the PV array. The partition is denoted by *n* subsets $\boldsymbol{B}_1$, $\boldsymbol{B}_2$, $\cdots$, and $\boldsymbol{B}_n$, which correspond to the *n* groups consisting of m_1, m_2, $\cdots$, and m_n PV cells, respectively. The subsets $\boldsymbol{B}_1$, $\boldsymbol{B}_2$, $\cdots$, and $\boldsymbol{B}_n$ satisfy

$$\cup_{j=1}^{n} \boldsymbol{B}_j = \boldsymbol{A}, \tag{2}$$

and

$$\boldsymbol{B}_j \cap \boldsymbol{B}_k = \emptyset, \text{ for } \forall\, j, k \in \{1, 2, \cdots, n\} \text{ and } j \neq k. \tag{3}$$

Furthermore, the integer values in subset $\boldsymbol{B}_j$ must be smaller than the integer values in subset $\boldsymbol{B}_k$, for any $1 \leq j < k \leq n$, due to the structural characteristics of the proposed reconfiguration technique. A partitioning satisfying the above properties is called an *alphabetical partitioning*.

3. PROBLEM FORMULATION

3.1 Problem Statement

The solar irradiance distribution over the PV array on the HEV changes over time, due to driving direction change and shading caused by buildings, clouds, and other moving vehicles. Temperature variation is also severe because of the engine heat dissipation and convection due to airflow. We should perform the PV array reconfiguration algorithm at every decision epoch t to maximize the PV system output power. For notational convenience, we drop the time index t. We denote the solar irradiance and PV cell temperature of the *i*-th $(1 \leq i \leq N)$ PV cell by G_i and T_i, respectively. We obtain G_i and T_i values using irradiance and temperature sensors in the system. We denote the output voltage and current of the *i*-th PV cell by $V_{pv,i}^{c}$ and $I_{pv,i}^{c}$, respectively. The PV array configuration $\mathcal{C}$ is the major control variable of the reconfiguration algorithm.

We develop V-I characteristic of the PV array with a configuration $\mathcal{C}(n;\ m_1, m_2, \cdots, m_n)$ that corresponds to the alphabetical partitioning $\boldsymbol{B}_1$, $\boldsymbol{B}_2$, $\cdots$, and $\boldsymbol{B}_n$ as follows. We use $V_{pv,j}^{g}$ to denote the output voltage of the *j*-th PV group, and use V_{pv} and I_{pv} to denote the output voltage and current of the PV array, respectively. The V_{pv} and I_{pv} values can be effectively controlled by the PV charger. From the Kirchhoff's laws, we have:

$$I_{pv} = \sum_{i \in \boldsymbol{B}_j} I_{pv,i}^{c},\ \forall\, j \in \{1, 2, \cdots, n\}, \tag{4}$$

$$V_{pv,j}^{g} = V_{pv,i}^{c}, \text{ for } \forall\, i \in \boldsymbol{B}_j \text{ and } j \in \{1, 2, \cdots, n\}, \tag{5}$$

and

$$V_{pv} = \sum_{j=1}^{n} V_{pv,j}^{g}. \tag{6}$$

We control and maintain the PV array operating point (V_{pv}, I_{pv}) using the PV charger. The power loss of the PV charger, P_{conv}, is calculated from its input voltage, input current, output voltage, and output current, i.e., V_{pv}, I_{pv}, V_{bat}, and I_{bat_pv}, respectively [11]. Due to the energy conservation law, we have:

$$V_{pv} \cdot I_{pv} = P_{conv} + V_{bat} \cdot I_{bat\_pv}, \tag{7}$$

where V_{bat} and I_{bat_pv} are the battery's terminal voltage and charging current from the PV system, respectively. The formal problem statement of the PV array reconfiguration (PAR) problem for HEV is described as follows:

PAR Problem Statement: Given the solar irradiance G_i and the temperature T_i of each *i*-th $(1 \leq i \leq N)$ PV cell in the PV array, and the battery terminal voltage V_{bat}, **find** the optimal PV array configuration $\mathcal{C}$ and the PV array operating point (V_{pv}, I_{pv}), **such that** the PV charger output current I_{bat_pv} is maximized.

3.2 Problem Decomposition

We propose a near-optimal solution to the PAR problem using a novel method that consists of a kernel algorithm, an MPTT control algorithm, and an outer loop finding the optimal number of PV groups in the PV array. The kernel algorithm finds the optimal PV array configuration such that all PV cells can work near their MPPs. The kernel algorithm derives the optimal PV array configuration $\mathcal{C}(n;\ m_1, m_2, \cdots, m_n)$ for a given n value to maximize the PV array MPP output power. The MPP output power of the PV array is the maximum achievable $V_{pv} \cdot I_{pv}$ value under a given solar irradiance and temperature distribution on the PV array, and a given PV array configuration. The subsequent MPTT control algorithm aims to find the optimal PV array operating point (V_{pv}, I_{pv}) taking into account the PV charger efficiency variation, such that I_{bat_pv} is maximized. We use the optimal PV array configuration $\mathcal{C}$ obtained via the kernel algorithm for the subsequent MPTT control algorithm. The outer loop enumerates all the possible n values $(1 \leq n \leq N)$ and finds the optimal one. The outline of this method is given in Algorithm 1. The next section describes the kernel algorithm in detail, which is the key part in Algorithm 1.

Algorithm 1: Near-Optimal Solution of the PAR Problem.

For each possible n value $(1 \leq n \leq N)$:

> Run the **kernel algorithm** to find the optimal PV array configuration $\mathcal{C}(n;\ m_1, m_2, \cdots, m_n)$, such that the PV array MPP output power is maximized.
>
> Run the **MPTT control algorithm** to find the optimal PV array operating point (V_{pv}, I_{pv}) that maximizes I_{bat_pv}, under the obtained optimal PV array configuration $\mathcal{C}(n;\ m_1, m_2, \cdots, m_n.)$
>
> The maximal PV charger output current is denoted by $I_{bat\_pv,n}^{max}$.

Find the optimal n value that maximizes $I_{bat\_pv,n}^{max}$, and the corresponding optimal PV array configuration $\mathcal{C}(n;\ m_1, m_2, \cdots, m_n)$ and PV array operating point (V_{pv}, I_{pv}).

4. THE KERNEL ALGORITHM

The maximum solar power that can be drawn from a PV array is the sum of MPP output power of all the PV cells in that array. Under the non-uniformity of solar irradiance and temperature, PV cells in a balanced *n*-by-*m* configuration can hardly operate at their MPPs simultaneously. Our reconfiguration technique aims at making all the PV cells operate at, or close to, their MPPs by updating the configuration of the PV array according to current solar irradiance and temperature distributions. In Figure 7, each PV cell is labeled with its MPP output voltage and current. If the PV array employs the $\mathcal{C}(3;5,3,4)$ configuration as shown in Figure 7, all PV cells work at their MPPs simultaneously with the PV array output voltage of 3.6 V (1.5+0.9+1.2=3.6 V) and output current of 4.5 A (1.5+1.5+1.5=4.5 A). The goal of our kernel algorithm is to find a configuration for the PV array such that (i) PV cells within the same PV group have very close MPP output voltages and (ii) the sum of MPP output currents of PV cells within the same group is quite similar among all the PV groups.

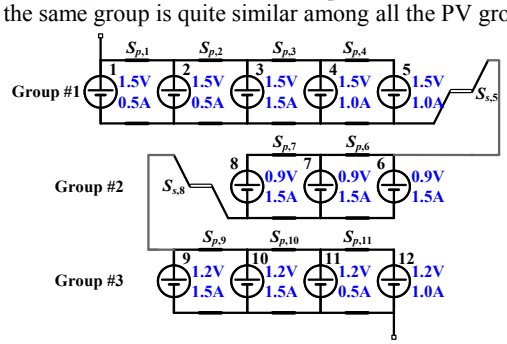

Figure 7. An illustration of the PV array reconfiguration.

4.1 Simplifying the Problem

The kernel algorithm finds the optimal PV array configuration to maximize the PV array MPP output power for the specified number of PV groups in the array. We name the problem *simplified PAR* (SPAR) problem. We further simplify the SPAR problem assuming *ideal PV cells*, and name the new problem *ideal PV Cell-based SPAR* (IC-SPAR) problem. The V-I characteristic of an ideal PV cell is a step function such that

$$I_{pv,i}^{c} = \begin{cases} I_{pv,i}^{c,MPP}, & \text{if } V_{pv,i}^{c} \le V_{pv,i}^{c,MPP} \\ 0, & \text{otherwise} \end{cases}, \tag{8}$$

where $V_{pv,i}^{c,MPP}$ and $I_{pv,i}^{c,MPP}$ denote the MPP output voltage and current of the *i*-th PV cell in the PV array, which are calculated from the solar irradiance G_i and temperature T_i. The ideal PV cell is an effective approximation of the real PV cell. We use $V_{pv,\mathrm{IC}}^{MPP}(\mathcal{C})$, $I_{pv,\mathrm{IC}}^{MPP}(\mathcal{C})$, and $P_{pv,\mathrm{IC}}^{MPP}(\mathcal{C})$ to denote the MPP output voltage, current, and power, respectively, of the ideal PV cell array with a configuration of $\mathcal{C}(n;\, m_1, m_2, \cdots, m_n)$. These values are calculated as:

$$V_{pv,\mathrm{IC}}^{MPP}(\mathcal{C}) = \sum_{j=1}^{n} \min_{i \in \boldsymbol{B}_j} V_{pv,i}^{c,MPP}, \tag{9}$$

$$I_{pv,\mathrm{IC}}^{MPP}(\mathcal{C}) = \min_{1 \le j \le n} \sum_{i \in \boldsymbol{B}_j} I_{pv,i}^{c,MPP}, \tag{10}$$

$$P_{pv,\mathrm{IC}}^{MPP}(\mathcal{C}) = \left(\sum_{j=1}^{n} \min_{i \in \boldsymbol{B}_j} V_{pv,i}^{c,MPP} \right) \cdot \left(\min_{1 \le j \le n} \sum_{i \in \boldsymbol{B}_j} I_{pv,i}^{c,MPP} \right). \tag{11}$$

Thus the IC-SPAR problem becomes: find the optimal array configuration $\mathcal{C}(n;\, m_1, m_2, \cdots, m_n)$ (corresponding to the optimal alphabetical partitioning $\boldsymbol{B}_1, \boldsymbol{B}_2, \cdots$, and $\boldsymbol{B}_n$) for a given n value, such that the $P_{pv,\mathrm{IC}}^{MPP}(\mathcal{C})$ value calculated from (11) is maximized.

4.2 The Pareto-Optimal Substructure

We consider a reduced-size PV array consisting of the first L ($L \le N$) PV cells of the original N-cell PV array. The reduced-size L-cell PV array is composed of l ($l \le n$) PV groups. We denote a possible configuration of the L-cell PV array by $\mathcal{C}^{L,l}$. Finding the optimal L-cell PV array configuration is equivalent to finding the optimal alphabetical partitioning $\boldsymbol{B}_1^{L,l}, \boldsymbol{B}_2^{L,l}, \cdots, \boldsymbol{B}_l^{L,l}$ of the set $\boldsymbol{A}^L = \{1, 2, \cdots, L\}$. The configuration is optimal when the MPP output power $P_{pv,\mathrm{IC}}^{MPP}(\mathcal{C}^{L,l}) = \left(\sum_{j=1}^{l} \min_{i \in \boldsymbol{B}_j^{L,l}} V_{pv,i}^{c,MPP} \right) \cdot \left(\min_{1 \le j \le l} \sum_{i \in \boldsymbol{B}_j^{L,l}} I_{pv,i}^{c,MPP} \right)$ is maximized. We use $V_{pv,\mathrm{IC}}^{MPP}(\mathcal{C}^{L,l}) = \sum_{j=1}^{l} \min_{i \in \boldsymbol{B}_j^{L,l}} V_{pv,i}^{c,MPP}$ and $I_{pv,\mathrm{IC}}^{MPP}(\mathcal{C}^{L,l}) = \min_{1 \le j \le l} \sum_{i \in \boldsymbol{B}_j^{L,l}} I_{pv,i}^{c,MPP}$ to denote the MPP output voltage and current of the PV array with configuration $\mathcal{C}^{L,l}$, respectively. We name the new problem the (L,l) *reconfiguration problem*. The more general (L,l) reconfiguration problem becomes the original IC-SPAR problem when $L = N$ and $l = n$. We find the Pareto-optimal substructure property of this (L,l) reconfiguration problem as follows.

Definition 1 (*Pareto superiority*): Consider two configurations $\mathcal{C}^{L,l}$ and $\hat{\mathcal{C}}^{L,l}$ of the (L,l) reconfiguration problem. Configuration $\mathcal{C}^{L,l}$ is Pareto-superior to $\hat{\mathcal{C}}^{L,l}$ if $V_{pv,\mathrm{IC}}^{MPP}(\mathcal{C}^{L,l}) > V_{pv,\mathrm{IC}}^{MPP}(\hat{\mathcal{C}}^{L,l})$ and $I_{pv,\mathrm{IC}}^{MPP}(\mathcal{C}^{L,l}) \ge I_{pv,\mathrm{IC}}^{MPP}(\hat{\mathcal{C}}^{L,l})$, or $V_{pv,\mathrm{IC}}^{MPP}(\mathcal{C}^{L,l}) \ge V_{pv,\mathrm{IC}}^{MPP}(\hat{\mathcal{C}}^{L,l})$ and $I_{pv,\mathrm{IC}}^{MPP}(\mathcal{C}^{L,l}) > I_{pv,\mathrm{IC}}^{MPP}(\hat{\mathcal{C}}^{L,l})$.

Definition 2 (*Pareto-optimal configuration* and *Pareto-optimal set*): A configuration $\mathcal{C}^{L,l}$ is a *Pareto-optimal configuration* of the (L,l) reconfiguration problem if no other configuration of the (L,l) reconfiguration problem is Pareto superior to $\mathcal{C}^{L,l}$. The set of all Pareto-optimal configurations of the (L,l) reconfiguration problem is the *Pareto-optimal* (*configuration*) *set* of the problem.

Next we present two theorems. Theorem 1 demonstrates that the optimal configuration of each (L,l) reconfiguration problem is an element in the Pareto-optimal set of that problem, whereas Theorem 2 provides the Pareto-optimal substructure property. Proofs are omitted due to limited space.

Theorem 1 (Optimal configuration and Pareto-optimal configurations): The optimal configuration $\mathcal{C}^{L,l}$ (with the maximum MPP output power $P_{pv,\mathrm{IC}}^{MPP}(\mathcal{C}^{L,l})$) of the (L,l) reconfiguration problem is an element in the Pareto-optimal set of the (L,l) reconfiguration problem.

Theorem 2 (The Pareto-optimal substructure): Suppose that a configuration $\mathcal{C}^{L,l}$, corresponding to an alphabetical partitioning $\boldsymbol{B}_1^{L,l}, \boldsymbol{B}_2^{L,l}, \cdots, \boldsymbol{B}_{l-1}^{L,l}, \boldsymbol{B}_l^{L,l}$, is a Pareto-optimal configuration of the (L,l) reconfiguration problem, and the last (the l-th) PV group consists of $m_l^{L,l}$ cells. Then the alphabetical partitioning $\boldsymbol{B}_1^{L,l}, \boldsymbol{B}_2^{L,l}, \cdots, \boldsymbol{B}_{l-1}^{L,l}$ (or the corresponding configuration) must also be Pareto-optimal in the $(L - m_l^{L,l}, l-1)$ reconfiguration problem.

4.3 The MCHV Function

Based on the above-described Pareto-optimal substructure property, one can find the optimal solution of the original IC-SPAR problem by storing the complete Pareto-optimal set of each (L,l) reconfiguration problem with $L \le N$ and $l \le n$, in a way similar to the conventional dynamic programming. However, cardinality of the Pareto-optimal set of the (L,l) reconfiguration problem could be in the order of $L!$, which implies that the Pareto-optimal set cardinality could be exponential. Hence, it is impractical to store the whole Pareto-optimal set of each (L,l) reconfiguration problem to solve the original IC-SPAR problem.

For effectively solving the IC-SPAR problem, we introduce a new function, named *maximal_current_higher_voltage* (MCHV) function for each (L,l) reconfiguration problem, denoted by $f_{MCHV}^{L,l}(V)$. The MCHV function $f_{MCHV}^{L,l}(V)$ derives the maximum $I_{pv,\mathrm{IC}}^{MPP}(\mathcal{C}^{L,l})$ value achieved by any configuration $\mathcal{C}^{L,l}$ of the (L,l) reconfiguration problem satisfying $V_{pv,\mathrm{IC}}^{MPP}(\mathcal{C}^{L,l}) \ge V$, i.e.,:

$$f_{MCHV}^{L,l}(V) = \max_{\mathcal{C}^{L,l}:\, V_{pv,\mathrm{IC}}^{MPP}(\mathcal{C}^{L,l}) \geq V} I_{pv,\mathrm{IC}}^{MPP}(\mathcal{C}^{L,l}). \quad (12)$$

If there exists no configuration $\mathcal{C}^{L,l}$ satisfying $V_{pv,\mathrm{IC}}^{MPP}(\mathcal{C}^{L,l}) \geq V$ for relatively large V values, we have $f_{MCHV}^{L,l}(V) = 0$. The domain of the MCHV function for the (L,l) reconfiguration problem is given by $[\hat{V}_{pv,\mathrm{IC},min}^{MPP,L,l}, \hat{V}_{pv,\mathrm{IC},max}^{MPP,L,l}]$, where $\hat{V}_{pv,\mathrm{IC},min}^{MPP,L,l}$ and $\hat{V}_{pv,\mathrm{IC},max}^{MPP,L,l}$ values are the estimated lower and upper bounds of the $V_{pv,\mathrm{IC}}^{MPP}(\mathcal{C}^{L,l})$ value for any configuration $\mathcal{C}^{L,l}$, respectively. The $\hat{V}_{pv,\mathrm{IC},min}^{MPP,L,l}$ and $\hat{V}_{pv,\mathrm{IC},max}^{MPP,L,l}$ values are calculated by

$$\hat{V}_{pv,\mathrm{IC},min}^{MPP,L,l} = l \cdot \min_{1 \leq i \leq L} V_{pv,i}^{c,MPP}, \quad (13)$$

$$\hat{V}_{pv,\mathrm{IC},max}^{MPP,L,l} = l \cdot \max_{1 \leq i \leq L} V_{pv,i}^{c,MPP}. \quad (14)$$

Finding tighter upper and lower bounds is an interesting problem, but it is outside the scope of the present paper. An illustration of the MCHV function is shown in Figure 8.

The MCHV function is a non-increasing function with a set of points of discontinuity. Each point of discontinuity in the MCHV function corresponds to a Pareto-optimal configuration of the (L,l) reconfiguration problem. Point $(V_a, f_{MCHV}^{L,l}(V_a))$ shown in Figure 8 corresponds to a Pareto-optimal configuration with $V_{pv,\mathrm{IC}}^{MPP}(\mathcal{C}^{L,l}) = V_a$ and $I_{pv,\mathrm{IC}}^{MPP}(\mathcal{C}^{L,l}) = f_{MCHV}^{L,l}(V_a)$, since we have $I_{pv,\mathrm{IC}}^{MPP}(\mathcal{C}^{L,l}) < f_{MCHV}^{L,l}(V_a)$ for any configuration of the (L,l) reconfiguration problem satisfying $V_{pv,\mathrm{IC}}^{MPP}(\mathcal{C}^{L,l}) > V_a$. Finally, the MCHV function of each (L,l) reconfiguration problem fully represents the Pareto-optimal set of that problem.

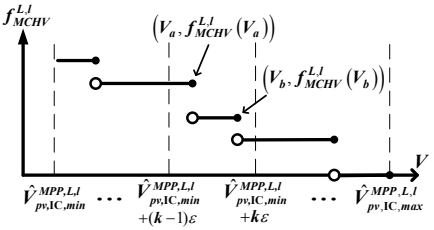

Figure 8. An illustration of the MCHV function.

4.4 Implementation of Kernel Algorithm

In the MCHV function for an (L,l) reconfiguration problem, the total number of points of discontinuity could also be exponential. Hence, we represent the MCHV function in discrete domain. We define a three-dimensional matrix **F_MCHV**, where $\mathbf{F\_MCHV}(L,l,k)$ $(1 \leq k \leq K+1)$ stores the $f_{MCHV}^{L,l}\big(\hat{V}_{pv,\mathrm{IC},min}^{MPP,L,l} + (k-1)\varepsilon\big)$ value. In the above expression, $\varepsilon = \frac{\hat{V}_{pv,\mathrm{IC},max}^{MPP,L,l} - \hat{V}_{pv,\mathrm{IC},min}^{MPP,L,l}}{K}$, and K is the predefined precision level in the kernel algorithm. When $K \to \infty$, the array $\mathbf{F\_MCHV}(L,l,k)$ $(1 \leq k \leq K+1)$ fully represents the MCHV function $f_{MCHV}^{L,l}(V)$, which is however not practical since the size of **F_MCHV** is infinite. When K is finite, the Pareto-optimal configurations of the (L,l) reconfiguration problem can be classified into two categories: *observable* and *unobservable* Pareto-optimal configurations. Consider a Pareto-optimal configuration $\mathcal{C}^{L,l}$ of the (L,l) reconfiguration problem satisfying $\hat{V}_{pv,\mathrm{IC},min}^{MPP,L,l} + (k-1)\varepsilon \leq V_{pv,\mathrm{IC}}^{MPP}(\mathcal{C}^{L,l}) < \hat{V}_{pv,\mathrm{IC},min}^{MPP,L,l} + k\varepsilon$. Then $\mathcal{C}^{L,l}$ is *observable* if $\mathbf{F\_MCHV}(L,l,k) = I_{pv,\mathrm{IC}}^{MPP}(\mathcal{C}^{L,l})$, and is *unobservable* otherwise (i.e., $\mathbf{F\_MCHV}(L,l,k) > I_{pv,\mathrm{IC}}^{MPP}(\mathcal{C}^{L,l})$.) An example of observable Pareto-optimal configuration is the one corresponding to the point $(V_a, f_{MCHV}^{L,l}(V_a))$ in Figure 8, and an example of unobservable Pareto-optimal configuration is the one corresponding to the point $(V_b, f_{MCHV}^{L,l}(V_b))$. The following lemma and theorem prove that we can find an approximate solution of the IC-SPAR problem by considering only the observable Pareto-optimal configurations in the kernel algorithm implementation.

Lemma 1 (Bound on MPP output power of unobservable Pareto-optimal configurations): For each unobservable Pareto-optimal configuration $\mathcal{C}^{L,l}$ of the (L,l) reconfiguration problem satisfying $\hat{V}_{pv,\mathrm{IC},min}^{MPP,L,l} + (k-1)\varepsilon \leq V_{pv,\mathrm{IC}}^{MPP}(\mathcal{C}^{L,l}) < \hat{V}_{pv,\mathrm{IC},min}^{MPP,L,l} + k\varepsilon$, there exists a corresponding observable Pareto-optimal configuration $\tilde{\mathcal{C}}^{L,l}$ with $\hat{V}_{pv,\mathrm{IC},min}^{MPP,L,l} + (k-1)\varepsilon \leq V_{pv,\mathrm{IC}}^{MPP}\big(\tilde{\mathcal{C}}^{L,l}\big) < V_{pv,\mathrm{IC}}^{MPP}(\mathcal{C}^{L,l})$ and $\mathbf{F\_MCHV}(L,l,k) = I_{pv,\mathrm{IC}}^{MPP}\big(\tilde{\mathcal{C}}^{L,l}\big) > I_{pv,\mathrm{IC}}^{MPP}(\mathcal{C}^{L,l})$. Besides, the MPP output power $P_{pv,\mathrm{IC}}^{MPP}(\mathcal{C}^{L,l})$ of the unobservable Pareto-optimal configuration $\mathcal{C}^{L,l}$ is bounded as follows:

$$P_{pv,\mathrm{IC}}^{MPP}(\mathcal{C}^{L,l}) \leq P_{pv,\mathrm{IC}}^{MPP}\big(\tilde{\mathcal{C}}^{L,l}\big) + \varepsilon \cdot I_{pv,\mathrm{IC}}^{MPP}\big(\tilde{\mathcal{C}}^{L,l}\big). \quad (15)$$

Theorem 3 (Approximate solution): We use $\mathcal{C}^{near\_opt}$ to denote the near-optimal solution (configuration) of the IC-SPAR problem obtained by considering only the observable Pareto-optimal configurations in the kernel algorithm implementation, with details shown in Algorithm 2. We use $\mathcal{C}^{opt}$ to denote the true optimal solution (configuration) of the IC-SPAR problem. Then the MPP output power $P_{pv,\mathrm{IC}}^{MPP}(\mathcal{C}^{near\_opt})$ of the near-optimal configuration $\mathcal{C}^{near\_opt}$ is bounded as follows:

$$P_{pv,\mathrm{IC}}^{MPP}(\mathcal{C}^{near\_opt}) \geq P_{pv,\mathrm{IC}}^{MPP}(\mathcal{C}^{opt}) \cdot \big(1 - B(K)\big), \quad (16)$$

where $B(K)$ is a function of the predefined parameter K and converges to 0 when $K \to \infty$.

Since the number of observable Pareto-optimal configurations for each (L,l) reconfiguration problem is bounded by K, practical implementation of the kernel algorithm is feasible. Details of the proposed dynamic programming based kernel algorithm to solve the IC-SPAR problem are provided in Algorithm 2. The solution of the IC-SPAR problem serves as the near-optimal solution of the SPAR problem, and the original PAR problem can be further solved using Algorithm 1.

Algorithm 2: The Kernel Algorithm.

Maintain three-dimensional matrices **F_MCHV**, **V_Pareto**, **Last_Par_1** and **Last_Par_2**. Each has N rows, n columns and $K+1$ layers.

Initialization:

$\mathbf{F\_MCHV}(L,1,k) \leftarrow \sum_{1 \leq i \leq L} I_{pv,i}^{c,MPP}$ and $\mathbf{V\_Pareto}(L,1,k) \leftarrow \min_{1 \leq i \leq L} V_{pv,i}^{c,MPP}$ for $1 \leq L \leq N$ and $1 \leq k \leq K+1$.

The rest of entries in all four matrices **F_MCHV**, **V_Pareto**, **Last_Par_1** and **Last_Par_2** are initialized to be zero.

For l from 2 to n:

  For L from l to N:

    Calculate $\hat{V}_{pv,\mathrm{IC},min}^{MPP,L,l}$ and $\hat{V}_{pv,\mathrm{IC},max}^{MPP,L,l}$ values using (13) and (14).

    Calculate ε using $\varepsilon = \frac{\hat{V}_{pv,\mathrm{IC},max}^{MPP,L,l} - \hat{V}_{pv,\mathrm{IC},min}^{MPP,L,l}}{K}$.

    For k from 1 to $K+1$:

      $\mathbf{F\_MCHV}(L,l,k) \leftarrow \max_{(l-1 \leq L_1 < L,\ 1 \leq k_1 \leq K+1)} I_{temp}(L_1,k_1)$,
      s.t. $V_{temp}(L_1,k_1) \geq \hat{V}_{pv,\mathrm{IC},min}^{MPP,L,l} + (k-1)\varepsilon$.

      In the above expressions:
      $V_{temp}(L_1,k_1) = \mathbf{V\_Pareto}(L_1, l-1, k_1) + \min_{L_1 < i \leq L} V_{pv,i}^{c,MPP}$,
      $I_{temp}(L_1,k_1) = \min\{\mathbf{F\_MCHV}(L_1, l-1, k_1), \sum_{L_1 < i \leq L} I_{pv,i}^{c,MPP}\}$.

      If $\mathbf{F\_MCHV}(L,l,k) > 0$:

        $(L_{opt}, k_{opt}) \leftarrow \mathrm{argmax}_{(l-1 \leq L_1 < L,\ 1 \leq k_1 \leq K+1)} I_{temp}(L_1,k_1)$,
        s.t. $V_{temp}(L_1,k_1) \geq \hat{V}_{pv,\mathrm{IC},min}^{MPP,L,l} + (k-1)\varepsilon$.

        $(\mathbf{Last\_Par\_1}(L,l,k), \mathbf{Last\_Par\_2}(L,l,k)) \leftarrow (L_{opt}, k_{opt})$.

        $\mathbf{V\_Pareto}(L,l,k) \leftarrow V_{temp}(L_{opt}, k_{opt})$.

The near-optimal MPP output power of the PV array can be calculated by $\max_{1 \leq k \leq K+1} \{\mathbf{V\_Pareto}(N,n,k) \cdot \mathbf{F\_MCHV}(N,n,k)\}$.

Trace back the three-dimensional matrices **Last_Par_1** and **Last_Par_2** to find the near-optimal configuration $\mathcal{C}^{near\_opt}$ of the PV array.

5. EXPERIMENTAL RESULTS

We compare the performances of two PV systems: one is the proposed system with reconfiguration technique, and the other is the baseline system without reconfiguration technique. Both PV systems contain a PV array of 60 PV cells, a charger and a battery bank. The PV array in the proposed system has the reconfiguration structure shown in Figure 5 while the PV array in the baseline system has a fixed 6x10 configuration, where 6 PV cell groups are connected in series and each PV group consists of 10 parallel-connected PV cells. The output power of baseline system is enhanced by the improved MPPT technique [4] and the integration of a bypass diode within each PV cell [6].

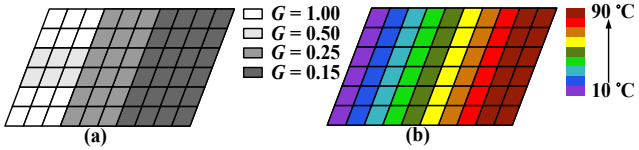

Figure 9. (a) Solar irradiance and (b) temperature distributions on the PV array.

We simulate the output power levels of the two systems under the solar irradiance and temperature distributions as shown in Figure 9. Although the mounting locations of PV cells in the proposed system are the same as those of PV cells in the baseline system, the PV array in the proposed system shows different configurations achieved by the reconfiguration technique, in response to different V_{bat} values. Table 1 summarizes the output power improvement of the proposed system compared to the baseline system with different battery terminal voltage V_{bat} values. The proposed system achieves up to 6X improvement in the output power level with the solar irradiance and temperature distributions as shown in Figure 9 when $V_{bat} = 45$ V. Table 1 also provides near-optimal configurations obtained from the proposed reconfiguration algorithm.

Table 1. Output power improvement of the proposed PV system with different V_{bat} values.

	V_{bat} (V)		
	15	30	45
PV array configuration	$\mathcal{C}$(9; 3, 12, 4, 4, 14, 4, 4, 12, 3)	$\mathcal{C}$(12; 2, 5, 10, 2, 3, 8, 8, 3, 2, 10, 5, 2)	$\mathcal{C}$(12; 2, 5, 10, 2, 3, 8, 8, 3, 2, 10, 5, 2)
Power output improvement	1.99X	2.71X	6.08X

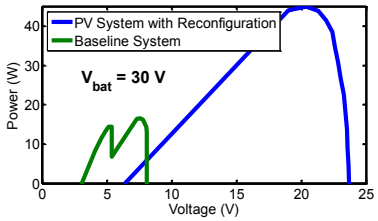

Figure 10. The V-P characteristics of the two PV systems.

In Figure 10, we plot the V-P characteristics of PV arrays in the proposed system and the baseline system with the irradiance and temperature distributions given in Figure 9 when $V_{bat} = 30$ V. The proposed system achieves significantly higher peak output power than that of the baseline system. Since the operating point of the PV array is always set to be its MPP to extract maximum output power out of the PV system, the proposed system outperforms the baseline system in Figure 10. Moreover, the V-P characteristic curve of the proposed system is unimodal even under irradiance and temperature non-uniformity with the proposed reconfiguration technique, while the V-P characteristic curve of the baseline system has multiple peaks. Therefore, the standard MPTT technique could be incorporated into the proposed system without extra modification. However, the MPPT or MPTT technique must be modified to track a global optimal operating point instead of a local optimal point in the baseline system. A typical modification would be searching the whole operating range of the PV array output voltage and current, which results in significantly higher time overhead compared with standard MPPT or MPTT technique based on the perturb and observe approach.

6. CONCLUSION

Non-uniformity of the solar irradiance and temperature on the PV array is a serious obstacle to efficient utilization of the PV system on HEV. This paper presents a dynamic PV array reconfiguration technique with systematic and scalable structural support and a dynamic programming based reconfiguration control algorithm. Experimental results demonstrate that the proposed reconfiguration method results in up to a factor of 6X output power level improvement compared with a baseline PV system.

ACKNOWLEDGEMENTS

This work is sponsored by a grant from the U.S. National Science Foundation, the Brain Korea 21 Project, the National Research Foundation of Korea (NRF) grant funded by the Korean Government (MEST) (No. 2011-0016480), and ICT at Seoul National University.

REFERENCES

[1] N. Femia, G. Petrone, G. Spagnuolo, and M. Vitelli, "Optimization of perturb and observe maximum power point tracking method," *IEEE Trans. on Power Electronics*, 2005.

[2] F. Liu, S. Duan, F. Liu, B. Liu, and Y. Kang, "A variable step size INC MPPT method for PV systems," *IEEE Trans. on Industrial Electronics*, 2008.

[3] Y. Kim, N. Chang, Y. Wang, and M. Pedram, "Maximum power transfer tracking for a photovoltaic-supercapacitor energy system," in *ISLPED*, 2010.

[4] H. Patel, and V. Agarwal, "Maximum power point tracking scheme for PV systems operating under partially shaded conditions," *IEEE Trans. on Industrial Electronics*, 2008.

[5] R. Bruendlinger, B. Bletterie, M. Milde, and H. Oldenkamp, "Maximum power point tracking performance under partially shaded PV array conditions," in *Proc. 21st EUPVSEC*, 2006.

[6] D. Nguyen, and B. Lehman, "An adaptive solar photovoltaic array using model-based reconfiguration algorithm," *IEEE Trans. on Industrial Electronics*, 2008.

[7] G. Velasco-Quesada, F. Guinjoan-Gispert, R. Pique-Lopez, M. Roman-Lumbreras, and A. Conesa-Rosa, "Electrical PV array reconfiguration strategy for energy extraction improvement in grid-connected PV systems," *IEEE Trans. on Industrial Electronics*, 2009.

[8] M. A. Chaaban, M. Alahmad, J. Neal, J. Shi, C. Berryman, Y. Cho, S. Lau, H. Li, A. Schwer, Z. Shen, J. Stansbury, and T. Zhang, "Adaptive photovoltaic system," in *IECON*, 2010.

[9] Y. Kim, S. Park, Y. Wang, Q. Xie, N. Chang, M. Poncino, and M. Pedram, "Balanced reconfiguration of storage banks in a hybrid electrical energy storage system," in *ICCAD*, 2011.

[10] W. Lee, Y. Kim, Y. Wang, N. Chang, M. Pedram, and S. Han, "Versatile high-fidelity photovoltaic module emulation system," in *ISLPED*, 2011.

[11] Y. Wang, Y. Kim, Q. Xie, N. Chang, and M. Pedram, "Charge migration efficiency optimization in hybrid electrical energy storage (HEES) systems," in *ISLPED*, 2011.